Measurement of the atomic Na(3P) lifetime and of retardation in the interaction between two atoms bound in a molecule

K. M. Jones†, P. S. Julienne, P. D. Lett, W. D. Phillips, E. Tiesinga, and C. J. Williams‡
Atomic Physics Division, PHYS A-167, National Institute of Standards and Technology, Gaithersburg, MD 20899 USA

Published in: Europhysics Letters, Vol. 35, p. 85-90 (1996)

From molecular spectroscopy of the Na_2 purely long-range 0_g^- state we determine the Na(3P) lifetime and measure the predicted but previously unobserved effect of retardation in the interaction between two atoms. Our lifetime $\tau(P_{3/2})$=16.230(16) ns helps to remove a longstanding discrepancy between experiment and theory. Electron cloud overlap is unimportant in the 0_g^- state ($R > 55a_0$) and the spectrum is calculated, *ab initio*, from atomic properties. By measuring the binding energies the 120 MHz correction due to retardation of the resonant dipole R^{-3} interaction is confirmed.

32.70.Fw, 32.80.Pj, 34.20.Cf

When two identical alkali atoms, one in the nS ground state and one in the optically excited nP state, are brought together to form a molecule, one of the resulting molecular potentials has a shallow well [1,2] at unusually large internuclear separations R ($\approx$70 Bohr radii, a_0, for Na_2). For the lighter alkalis, atoms bound in this purely long-range 0_g^- potential stay so far apart that the potential is completely determined by long-range forces and the atomic spin orbit splitting, and can thus be calculated with high precision. The dominant long-range interaction is the R^{-3} resonant dipole interaction, the strength of which is determined by the same atomic matrix element as the nP radiative lifetime. Using photoassociation spectroscopy of laser cooled atoms, we have measured absolute binding energies of the Na_2 0_g^- rovibrational levels to $\approx$ 5 MHz. This data allows us to make the most accurate determination yet of the Na(3P) atomic lifetime. Moreover, the observed binding energies can only be accounted for when the $\approx$100 MHz contribution due to the retardation of the resonant dipole interaction is included.

A longstanding $\approx$1% discrepancy between theory and experiment [4] for the Na(3P) lifetime has motivated several recent experiments [5–7], including our own. Molecular-spectroscopic atomic lifetime determinations [3,5,8–10], such as reported here, offer a new approach with sources of error different from the traditional direct methods involved in this discrepancy. Other precision molecular-spectroscopic determinations have used deeply bound electronic states [5,10]. In contrast, we use the purely long-range 0_g^- state and avoid the uncertainties associated with the potential in the short-range chemical-binding region.

In 1948 Casimir and Polder showed [11] that the finite propagation speed of light modifies the long-range forces between atoms. In particular they showed that the second order interaction that leads to the R^{-6} van der Waals potential between two ground state atoms becomes R^{-7} at large R. Although there has been no experimental confirmation of the effect between individual atoms, the corresponding retarded interactions between two atomically flat mica surfaces [12], a thin film of liquid helium and a surface [13], and between an atom and surfaces [14] have been measured quantitatively. Modification of the He Rydberg levels by retardation of the electron-core interaction has also been observed [15]. In spite of much theoretical discussion, no effect of retardation on molecular spectra has ever been reported. Retardation should alter the binding energy of $^4He_2$ by 10% [16], but this small (+3 MHz) effect remains unobserved. Here we observe retardation corrections of the first order, R^{-3}, resonant dipole interaction between identical ground and excited state atoms, first calculated in Ref. [17]. Extending the theory on the 0_g^- state to include retardation shows that this state is ideal for observing retardation since it can be cleanly separated from changes in the value of C_3.

Detailed spectroscopy of the alkali dimer purely long-range states has been made possible by the development of photoassociation of laser cooled atoms [3,8,9]. Since the atoms have small kinetic energy ($E/k_B \approx 500\,\mu K$), the Franck-Condon principle favors production of rovibrational levels near the molecular dissociation limit and the resolution of the technique ($k_BT/h \approx 10$MHz) is comparable to the natural linewidth of the molecular lines in question here (20 MHz). Because we start with free Na atoms we directly measure the binding energies of the molecular levels relative to the 3S + 3P asymptote.

Our analysis starts with the simple analytical model introduced by Movre and Pichler (M-P) [1]. They showed that the two 0_g^- potentials dissociating to 3S + 3P can be described as a spin-orbit avoided crossing between two Hund's case (a) basis states: a repulsive $^3\Pi_{0g}$ potential which goes as $+C_3/R^3$ and an attractive $^3\Sigma_{0g}$ potential which goes as $-2C_3/R^3$. The two adiabatic 0_g^- potentials are found by diagonalizing the potential matrix:

$$V_{MP} = \begin{array}{c} \\ \\ \end{array}\begin{array}{cc} \Pi & \Sigma \\ \left(\begin{array}{cc} \frac{C_3}{R^3} - \frac{2\Delta}{3} & \frac{\sqrt{2}\Delta}{3} \\ \frac{\sqrt{2}\Delta}{3} & -\frac{2C_3}{R^3} - \frac{\Delta}{3} \end{array}\right) & \begin{array}{c}\Pi \\ \Sigma\end{array} \end{array}, \qquad (1)$$

where Δ is the atomic spin-orbit splitting (Δ=515.520 GHz for Na) and the zero of energy is the S + $P_{3/2}$ asymptote. The upper 0_g^- potential has a shallow well and is shown in Figure 1a. The well depth is $\Delta/9$,

FIG. 1. a) The solid curve is the 0_g^- potential, in the M-P approximation, of Eq. (1) as a function of internuclear separation R. The dotted curve is the R-dependent correction to the 0_g^- potential (magnified $\times 100$) due to the retardation of the resonant dipole interaction. b) Mixing of the parent Σ and Π states of the 0_g^- potential as a function of R.

independent of C_3, and the potential minimum is at $R_e = (9C_3/2\Delta)^{1/3} \approx 71\,a_0$ for Na_2. The 0_g^- state is an R-dependent mixture of the Hund's case (a) states, $|0_g^-, R\rangle = b_\Pi(R)|\Pi\rangle + b_\Sigma(R)|\Sigma\rangle$, as shown in Fig. 1b.

The retardation of the resonant dipole interaction depends on the relative orientation of the atomic dipoles and is thus different for Σ and Π states [17]. The characteristic distance scale $\lambda\!\!\!^{-} = \lambda/2\pi = 1772\ a_0$ for Na is set by the 3S $\rightarrow$ 3P wavelength. Retardation is introduced into Eq. (1) by replacing C_3 by $C_3(1 + f_{\Sigma/\Pi}(R))$ [17], where, to lowest-order in $R/\lambda\!\!\!^{-}$, the corrections for the $^3\Sigma$ and $^3\Pi$ states are $f_\Sigma(R) = -f_\Pi(R) = (R/\lambda\!\!\!^{-})^2/2$. The resulting change in the 0_g^- potential is shown in Figure 1a. At R_e, where the 0_g^- state is 2/3 $^3\Pi_g$ character and 1/3 $^3\Sigma_g$ character, retardation increases the well depth by $(4/27)\Delta(R_e/\lambda\!\!\!^{-})^2 = 123$ MHz for Na_2. Since the dominant effect of retardation is to increase the well depth, measurements of the binding energies of low-lying vibrational levels are sensitive to retardation and relatively insensitive to the value of C_3. In contrast, the vibrational spacing is sensitive to the value of C_3 and only slightly affected by retardation.

To measure the effect of retardation, we need to understand all other effects that might be of similar magnitude. We present a perturbation theory calculation starting from the two state M-P model. We can write the total rovibrational energy as

$$E_{vJ} = E_v^{MP} + E_0 + B_v J(J+1) + \epsilon_v^{ret} + \epsilon_v^{disp} + \epsilon_v^{na} + \epsilon_v^{j^2} \quad (2)$$

where E_v^{MP} is the energy of the vibrational level v of the adiabatic 0_g^- potential shown in Fig. 1a; E_0 sets the zero of energy; B_v is the rotational constant $\langle 1/2\mu R^2\rangle$ (μ is the reduced mass); and the ϵ_v^x are the expectation values for the retardation correction (ret), dispersion interaction (disp), diagonal nonadiabatic corrections (na), and the J=0 rotational energy (j^2), as described below.

Table 1 gives the results of the perturbation calculation, using a value of C_3 discussed below. Calculation of the ϵ_v^x terms requires knowledge of the adiabatic vibrational wavefunction $\Psi_v(R)$ and the R-dependent $\Sigma - \Pi$ mixing. For example, the dispersion term is:

$$\epsilon_v^{disp} = \langle\Psi_v|b_\Pi^2(R)\{C_6^\Pi/R^6 + C_8^\Pi/R^8\} + b_\Sigma^2(R)\{C_6^\Sigma/R^6 + C_8^\Sigma/R^8\}|\Psi_v\rangle. \quad (3)$$

We use the dispersion coefficients of Ref. [18] and find the C_8 contribution to ϵ_v^{disp} is $< 3\%$. The retardation term is calculated using the full expression of Ref. [17]. It agrees well with the simple estimate given below Eq. (1) for v=0.

The diagonal non-adiabatic correction is due to the breakdown of the Born-Oppenheimer (fixed-nuclei) approximation as the potential changes character from Σ to Π [19], and arises because the kinetic energy operator is not diagonal in the adiabatic $|0_g^-, R\rangle$ basis, which diagonalizes Eq. (1). $\epsilon_v^{j^2}$ is the mechanical rotational en-

TABLE I. Binding energies of the 0_g^- state. v is the vibrational quantum number. $E_v^{MP} + E_0$ gives the energies (all energies are given in GHz) from the Movre-Pichler model of Eq. (1) using $C_3 = 6.219$ a.u.. The M-P model dissociates to the hyperfine barycenter of the 3S + 3P asymptotes. Our energies are referenced to the S(F=2) + $P_{3/2}$(F=3) hyperfine component (E_0 = 0.7071 GHz in Eq. (2)). Columns 3-7 give the perturbation estimates of the terms in Eq. (2). $E_{v\,J=2}$ sums the columns 2-6 plus $6B_v$, to get the energy of the J=2 state. The experimental J=2 and J=4 line positions are given in columns 10 and 11. The column labeled "theory" gives the energies from the diagonalization of the full Hamiltonian, as discussed in the text. Finally, the shifts caused by a +5% change in C_6^Σ and C_6^Π, and a +0.5% change in C_3 are given.

v	$E_v^{MP} + E_0$	ϵ_v^{ret}	ϵ_v^{disp}	ϵ_v^{na}	$\epsilon_v^{j^2}$	B_v	$E_{v\,J=2}$	theory J=2	exp. J=2	exp. J=4	+5% C_6	+0.5% C_3
0	-54.299	-0.121	-0.158	0.026	0.162	0.0303	-54.210	-54.207(3)	-54.208(5)	-53.786(5)	-0.008	-0.006
1	-47.437	-0.119	-0.145	0.022	0.152	0.0285	-47.356	-47.352(4)	-47.351(5)	-46.951(5)	-0.007	-0.016
2	-41.243	-0.116	-0.132	0.019	0.143	0.0266	-41.170	-41.165(5)	-41.164(5)	-40.790(5)	-0.007	-0.024
3	-35.682	-0.113	-0.119	0.016	0.134	0.0248	-35.616	-35.610(6)	-35.610(5)	-35.261(5)	-0.006	-0.031
4	-30.716	-0.110	-0.107	0.014	0.124	0.0230	-30.657	-30.649(7)	-30.652(5)	-30.329(5)	-0.005	-0.035
5	-26.306	-0.106	-0.095	0.012	0.115	0.0212	-26.253	-26.243(9)	-26.245(5)	-25.945(5)	-0.005	-0.038
6	-22.411	-0.103	-0.084	0.010	0.106	0.0195	-22.365	-22.353(10)	-22.353(5)	-22.074(5)	-0.004	-0.040

ergy of the total angular momentum J=0 state. Because the constituent atoms have internal angular momentum, the J=0 state of the molecule has non-zero mechanical rotation: $\vec{J} = \vec{\ell} + \vec{j}$ where $\vec{j} = \vec{j}_a + \vec{j}_b$, is the sum of the total angular momenta of the individual atoms. Thus the J=0 feature is a superposition of ℓ-states and its mechanical rotational energy can be evaluated from $\langle \mathrm{j}^2/2\mu\mathrm{R}^2\rangle (= \langle \ell^2/2\mu\mathrm{R}^2\rangle)$ using the known atomic composition of the Σ and Π basis states.

For comparison to the experimental data, we have also done a nonperturbative calculation [20], that includes the rotational (Coriolis) coupling and hyperfine interactions that mix the 0_g^- states with other nearby states. We start from the full Hamiltonian for all states correlating to 3S + 3P and include the terms discussed above plus an asymptotic approximation for the hyperfine interaction, the exact mechanical rotation operator, and a spin-spin magnetic dipole term. At $\mathrm{R} \approx 35$ a_0 the long-range potentials are fitted smoothly onto the *ab initio* potentials of [21]. We numerically calculate the rovibrational-hyperfine eigenvalues of this Hamiltonian. Uncertainties in the *ab initio* potentials have no effect on the 0_g^- level positions: replacing them with a hard wall at 30 a_0 gives no significant shift(< 1 MHz).

The experimental signals are largest for the J=2 feature of each vibrational level. This feature consists of 8 hyperfine sublevels with a spread of 5 MHz for v=0, rising to 22 MHz for v=6. Experimentally we do not resolve the hyperfine structure for these vibrational levels and, in the absence of a theoretical treatment of the hyperfine transition strengths, the theoretical energies reported in Table 1 are taken as the center of the spread of hyperfine lines and assigned an uncertainty of half of this spread.

We use a Zeeman slowed atomic beam to continuously feed Na atoms into a "dark spot" magneto-optical trap (MOT) [3]. This puts most of the atoms in the 3S(F=1) state. As shown in the inset to Figure 2 we produce and detect 0_g^- molecules by a two step photoassociative ionization process [8,22]. This technique has a higher signal-to-noise ratio than single-frequency trap loss techniques. Moreover, the trap loss technique shows no v=0 and 1 features because of the small vibrational kinetic energy of these states.

To obtain the rotational progression for a single vibrational state the photoassociating laser is scanned over ≈ 2 GHz while the ionizing laser is fixed. The total energy of the two photons is typically $\gtrsim 3$ GHz above the ionization threshold [8,22]. Na_2^+ ions are detected with a channel electron multiplier. Every $\approx 10\mu$sec we switch between a trapping phase with only the MOT lasers present, and a probe phase with only the photoassociating and ionizing lasers present. A counter is gated to receive only ions produced during the probe phase. The ionizing laser is at a frequency some tens of GHz above the atomic resonance, so that no ion signal is produced in the absence of the photoassociating laser. The two probe laser powers are set at a level where ac Stark shifts and power broadening of the lines are insignificant; consequently the trap loss is never more than $\approx 3\%$. Figure 2 shows the spectrum of the v=0 state.

FIG. 2. Ion signal versus photoassociating laser frequency for v=0 of the 0_g^- state. The solid curve is a fit of an s + d-wave Wigner-law lineshape of Ref. [23] to the respective peaks using $\mathrm{k_B T/h} = 9$ MHz and $\gamma = 22$ MHz. The arrow indicates the positions of the resonances. The inset shows the two-step photoassociative ionization procedure. The first photon has a variable frequency and produces a bound excited molecule from cold colliding atoms. The second photon, with fixed frequency, excites the molecule to a continuum of autoionizing states [8,22]. The frequency zero is a reference etalon fringe at 16971.6462 cm^{-1}.

Our spectra are calibrated by a 0.3 GHz free spectral range confocal etalon, locked to the saturated absorption spectrum of Na. For each data set we measure the lock point with respect to the atomic S(F=1) $\rightarrow$ $\mathrm{P}_{3/2}$(F=2) transition in the cold atom sample.

The peaks of spectral lines observed in photoassociation spectroscopy are not centered on the transition but are offset to the red by an energy of order $\mathrm{k}_B\mathrm{T}$ [23]. The temperature and the selection rules for the 0_g^- state [20] dictate that the J=2 lines will be predominantly due to the s- and d-wave channels (for $\mathrm{v} > 0$ only the s-wave is significant) while the J=4 lines are due to the d-wave channel. To extract the experimental line positions given in Table 1, we compare the data to a calculated lineshape assuming a simple thermally-averaged Wigner threshold law [23]. We fit the data to a single threshold with a common $\mathrm{k_B T/h} \approx 9$ MHz and a variable linewidth γ_v, which is greater than the molecular natural linewidth of 20 MHz in order to account for unresolved hyperfine structure. The quoted experimental uncertainties are dominated by determination of the etalon lock point and the temperature, which are common to all lines.

Table 1 shows that the measured binding energies are well reproduced by the calculations. The agreement is better than the uncertainties because of the commonality of sources of uncertainties. If retardation were to be neglected, the data could be fit only by making an unrealistically large change in C_6 ($\approx +75\%$) and a simultaneous change in C_3 (+0.4%). The calculated C_6

coefficients, on the other hand, are expected to be accurate to $\approx 5\%$ [18]. With retardation properly included we extract a value of $C_3 = 4.018(4)$ zJ·nm^3 (6.219(6) a.u.), where the numbers in parentheses are combined standard uncertainties (estimated standard deviations) from a numerical fit to the J=2 data, adding the experimental and theoretical uncertainties for each vibrational level in quadrature. The C_6^{Σ} and C_6^{Π} coefficients were determined by the fit (with the constant ratio from Ref. [18]) in the fit and were found to be consistent with the values from Ref. [18] to well within their 3.5% uncertainty from the fit. A fit to the J=4 positions is consistent, but with slightly larger uncertainties. Since in atomic units C_3 is equal to the square of the transition dipole matrix element and hence, inversely proportional to the atomic Na(3P) state lifetime, we can convert from C_3 to atomic lifetime to find $\tau(P_{3/2}) = 16.230(16)$ ns and $\tau(P_{1/2}) = 16.280(16)$ ns. We have used the fact that the difference between the $P_{1/2}$ and $P_{3/2}$ dipole matrix elements is negligible at this level of accuracy [24]. Our values agree with other new measurements (converted to $\tau(P_{3/2})$): decay in a fast atomic beam (16.254(22) ns) [6], a direct measurement of the atomic linewidth (16.237(35) ns) [7], and molecular spectroscopy of the A state of Na_2 (16.222(53) ns) [5] and also with recent theory (16.236 ns) [4], and (16.253 ns) [25]. The agreement between these techniques suggests that the systematic errors in previous fast beam measurements [26] are now eliminated.

We have estimated the size of the retardation contribution to the well depth for the 0_g^- purely long-range states in the other alkali dimers: Rb_2, 210 MHz (at $R_e = 34$ a_0); K_2, 134 MHz (at 54 a_0); Li_2, 24 MHz (at 255 a_0). For Rb_2, the current uncertainties in C_6 and C_8 make the effect difficult to detect. For Cs_2 we expect chemical binding effects to be large.

Using photoassociation spectroscopy, we have measured the binding energies of rovibrational levels in the 0_g^- purely long-range potential in Na_2 and shown that we can understand these energies in detail, including the shifts due to retardation of the resonant dipole interaction. Using the C_6's with 5% uncertainty from Ref. [18], we have measured the v=0 retardation shift to be 122(10) MHz, in good agreement with the predicted shift of 121 MHz. We have also determined the Na(3P) state lifetimes to 0.1%. Calculations of the hyperfine transition strengths, which depend on the details of the ground state potential, will allow us to reduce the uncertainties and put tighter constraints on the lifetime.

Since the submission of this manuscript we have learned of another precision molecular-spectroscopic atomic lifetime measurement (using Li) in which retardation effects can be observed [27].

We thank the US Office of Naval Research and the US Army Research Office for financial support. We also thank C. Sansonetti for valuable discussions, T. Brage, C. Froese Fischer, E. Tiemann, U. Volz, and J. Hall for communicating their results prior to publication, and L. Ratliff for contributions to the early stages of the experiment.

---

† Permanent address: Williams College, Williamstown, MA 01267

‡ Permanent address: James Franck Institute, University of Chicago, Chicago, IL 60637

[1] M. Movre and G. Pichler, J. Phys. B **10**, 2631 (1977).
[2] W. C. Stwalley, Y.-H. Uang and G. Pichler, Phys. Rev. Lett. **41**, 1164 (1978).
[3] L. P. Ratliff, et al., J. Chem. Phys. **101**, 2638 (1994).
[4] T. Brage and C. Froese-Fischer, Phys. Rev. A **49**, 2181 (1994); here the relativistically-corrected number is quoted (T. Brage, private communication, 1995).
[5] E. Tiemann, H. Knoeckel and H. Richling, submitted, (1996).
[6] U. Volz, M. Majerus, H. Liebel, A. Schmitt, and H. Schmoranzer, Phys. Rev. Lett., (accepted, 1996).
[7] C. Oates, K. Vogel and J. Hall, Phys. Rev. Lett., (accepted, 1996).
[8] P. D. Lett, P. S. Julienne and W. D. Phillips, Annu. Rev. Phys. Chem. **46**, 423 (1995).
[9] R. A. Cline, J. D. Miller, and D. J. Heinzen, Phys. Rev. Lett. **73**, 632 (1994).
[10] W. McAlexander, et al., Phys. Rev. A **51**, R871 (1995).
[11] H. Casimir and D. Polder, Phys. Rev.**73**, 360 (1948).
[12] J. Israelachvili and D. Tabor, Proc. Roy. Soc. (London) A331, **19** (1972), and references contained therein.
[13] C. Anderson and E. Sabisky, Phys. Rev. Lett. **24**, 1049 (1970).
[14] C. Sukenik, et al., Phys. Rev. Lett. **70**, 560 (1993).
[15] F. Levin and D. Micha, Eds., *Long-Range Casimir Forces, Theory and Recent Experiments on Atomic Systems* (Plenum, New York, 1993); N. Claytor, E. Hessels and S. Lundeen, Phys. Rev. A **52**, 165 (1995).
[16] F. Luo, et al., J. Chem. Phys. **98**, 9687 (1993).
[17] R. McLone and E. Power, Mathematika **11**, 91 (1964); W. J. Meath, J. Chem. Phys. **48**, 227 (1968).
[18] M. Marinescu and A. Dalgarno, Phys. Rev. A **52**, 311 (1995) and A. Dalgarno, private communication.
[19] F. Mies, Molec. Phys. **54**, 1423 (1985).
[20] C. J. Williams, E. Tiesinga and P. J. Julienne, Phys. Rev. A (in press), (1996).
[21] S. Magnier, et al., J. Chem. Phys. **98**, 7113 (1993), and private communication.
[22] P. D. Lett, et al. in *Resonance Ionization Spectroscopy* 1994, H.-J. Kluge, J. E. Parks, and K. Wendt, Eds. AIP Conference Proceedings **329**, pp. 289 (1995).
[23] R. Napolitano, et al., Phys. Rev. Lett. **73**, 1352 (1994).
[24] Y.-K. Kim, private communication (1995).
[25] P. Jonsson, A. Ynnerman, C. Froese Fischer, M. Godefroid and J. Olsen, Phys. Rev. A (submitted), (1995).
[26] A. Gaupp, P. Kuske, and H. J. Andrä, Phys. Rev. A **26**, 3351 (1982); H. Schmoranzer, D. Schulze-Hagenest, and S. A. Kandela, Symposium on Atomic Spectroscopy (SAS-79), Tuscon, Arizona (1979).
[27] W. I. McAlexander, E. R. I. Abraham, and R. G. Hulet, submitted, (1996).

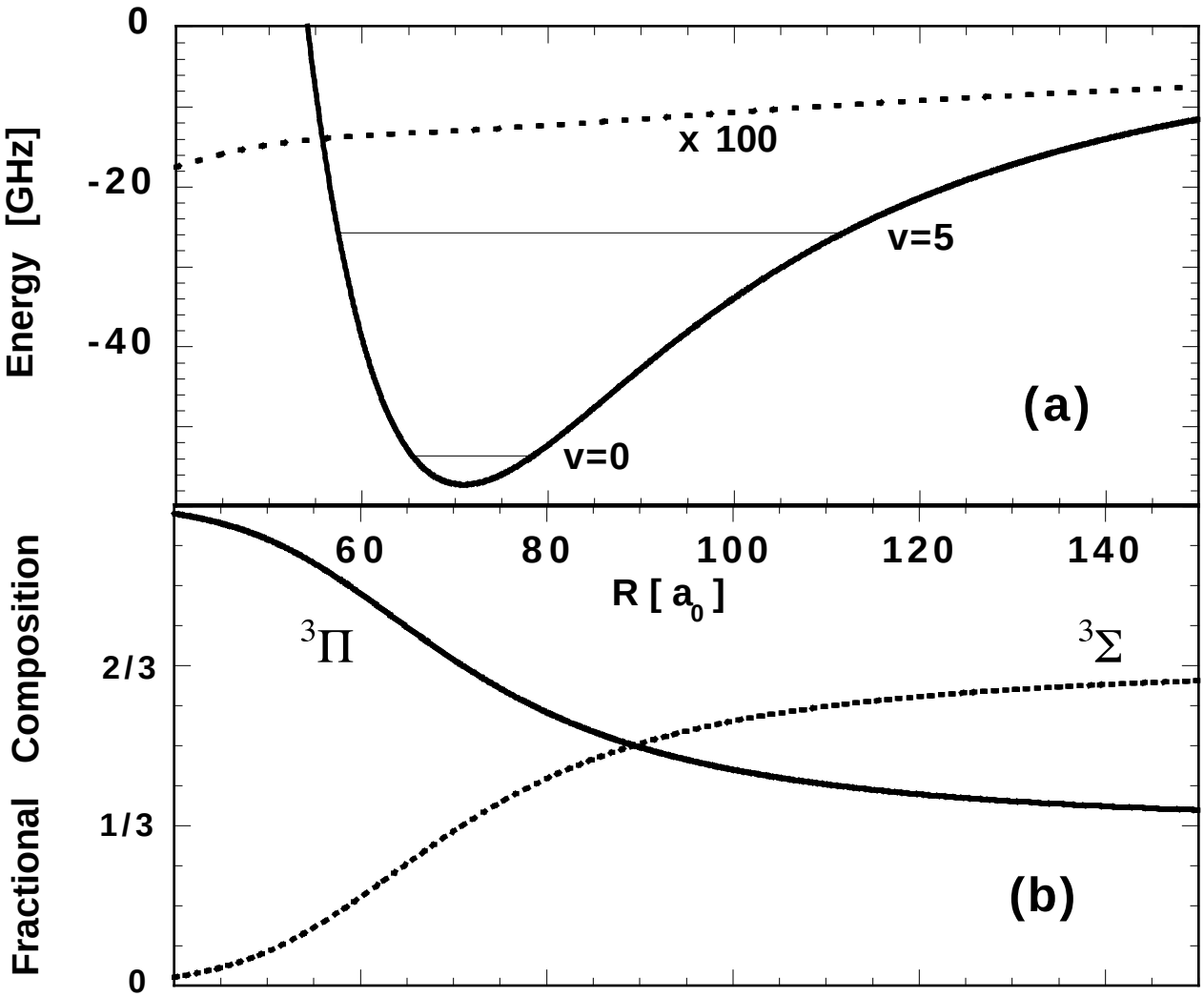
0
-20
-40
Energy [GHz]
x 100
v=5
v=0
(a)
60
80
100
120
140
R [a0]
Fractional Composition
2/3
1/3
0
3Π
3Σ
(b)

Figure 1

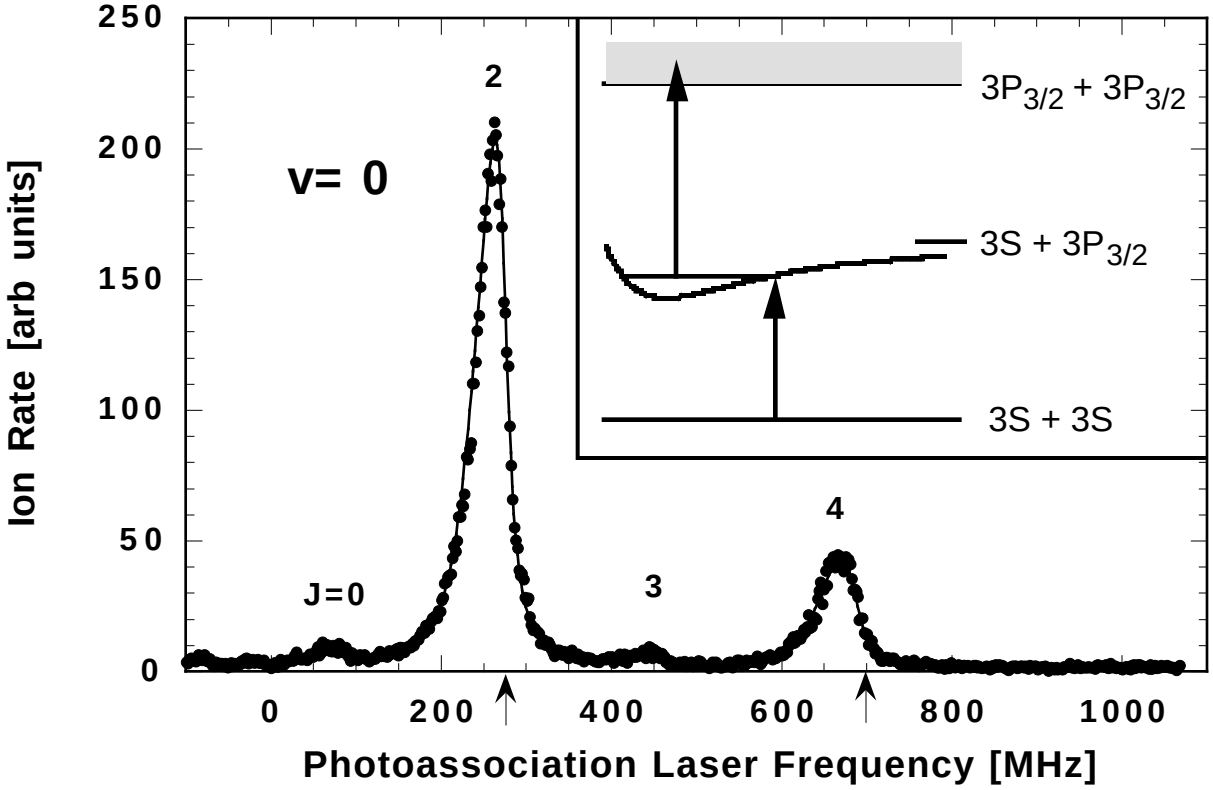
250
200
150
100
50
0
Ion Rate [arb units]
v= 0
2
J=0
3
4
0
200
400
600
800
1000
Photoassociation Laser Frequency [MHz]
3P3/2 + 3P3/2
3S + 3P3/2
3S + 3S

Figure 2